Int J Adv Manuf Technol (2018) 94:1317–1325
DOI 10.1007/s00170-017-0993-7

ORIGINAL ARTICLE

Residual stress and springback analysis for 304 stainless steel tubes in flexible-bending process

Yongping Zhou[1] · **Pengfei Li**[1] · **Mingzhe Li**[1] · **Liyan Wang**[1] · **Shuo Sun**[1]

Received: 19 April 2017 / Accepted: 16 August 2017 / Published online: 26 August 2017

Abstract Flexible-bending is an innovative processing technique for profiles and tubes, which adjusts the curved shape of the forming part through numerical control. In this article, the flexible-bending forming precision of 304 stainless steel tubes was studied. The flexible-bending process of the tubes was simulated through finite element method in comparison with that of experiments. After the investigations of forming springback and residual stress, we conclude that regardless of changes in wall thickness or outer diameter, the residual stress decreases first and then increases following the increase of the ratio between outer diameter and wall thickness. Neither the wall thickening rate nor thinning rate is affected by wall thickness changes. The thrust of the pusher maintains stable during the bending process. The changes of both wall thickness and outer diameter affect the springback to some extents. When the radius of the target is constant, the springback can be optimized by adjusting the offset of the bending die and the distance between the guide and the die. The experiments agree well with the numerical simulations.

Keywords Flexible-bending · Residual stress · Springback · Forming precision

1 Introduction

With excellent performance and durability, 304 stainless steel tubes are used as raw materials of environmental protection pipeline facilities. The bending forming of 304 stainless steel tubes has been widely used in medical engineering, petrochemical industry, urban/residential construction, automotive manufacturing, and aerospace industry, where bent profiles and tubes of different bending radii are needed [1–4]. Although a new roll-bending process that uses six transportation rolls and a roll-based bending head can realize three-dimensional (3D) bending of profiles [5], its composition and controlling method are comparatively complicated. As reported, the design of a three-roll tube bending process under geometrical uncertainties was improved [6]. R Gemignani wrote a patent on tube bending equipment [7]. A finite element model of the three-roll push-bending process which took all relevant influences (e.g., friction and machine stiffness) into consideration was developed [8]. In this paper, the flexible-bending computer numerical control (CNC) equipment was used. The flexible-bending is an innovative 3D bending technology for tubes and profiles. Figure 1 illustrates the principle of flexible-bending. Theoretically, the pusher controlled by a hydraulic servo motor pushes the tube along the Z-direction, while the guide is fixed. The inclination of the bending die is realized by changing the X- and Y-direction displacements of the bearing sleeve of the bending die. The distance between the deviation AB of the bending die is changed, but its horizontal distance L remains unchanged. That is, point B moves in the X-Y plane. Gantner et al. used active tilt with a certain angle in the bending die [9], and Li Pengfei et al. used Jilin University CNC flexible-bending machine [10]. Specifically, Li Pengfei et al. studied the small bending coefficient of the tube [10]. Compared with traditional bending techniques, the flexible-bending has some advantages, such as free definable bending geometry, and avoidance of re-clamping [11]. With the flexible-bending process, Murata studied the CNC bending system with pipes of different shapes and radii, and investigated the influence of process

✉ Mingzhe Li
limz@jlu.edu.cn

[1] Dieless Forming Technology Center, Jilin University, Changchun 130022, China

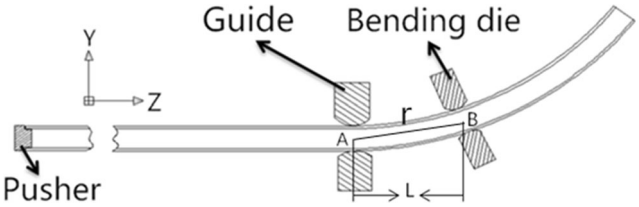

Fig. 1 Schematic of flexible-bending

parameters including the material properties, wall thickness, and inclination of the bending die [12, 13]. The result of flexible-bending is decided by the offset of the bending die [14], but the final geometry of the rotary draw bending process is determined by the geometry of the bending die [15, 16]. Gantner studied the flexible-bending with geometric shapes of continuous bending and spline bending and used free-bending to form a free definable bending geometry with transitionless bend-in-bends and spline bends [17], which is based on the same principle of MOS bending. Gantner also presented a five-axis bending model to show the development of free-bending, and used a kinematic model and a mathematic model to determine the movement curves of the bend die during free-bending [18]. However, after unloading, the springback affecting the geometrical precision of the forming part and the residual stress affecting the forming quality occur. These phenomena have never been studied in the flexible-bending process, and thus should be analyzed to find a solution to decrease or even eliminate springback.

In this study, we investigated the flexible-bending of 304 stainless steel tubes. The springback and residual stress of tubes were analyzed under different bending conditions through both simulations and experiments. The flexible-bending technique can be used to bend stainless steel tubes under different conditions. Regardless of changes in wall thickness or outer diameter, the ratio D/T between the outer diameter and wall thickness impacts the axial and circumferential residual stresses of the tubes. With the change of wall thickness, the wall thickening and thinning rates basically remain stable. During the bending process, the thrust of the pusher is steady. The changes of wall thickness and outer diameter also modestly impact springback. Under the constant target radius, springback is optimized by adjusting the offset of the bending die and its distance from the guide. The experiments agree well with the numerical simulations.

2 Experimental model

The experimental model was CNC flexible-bending machine developed by Jilin University (Fig. 2). The horizontal distance L between the guide and the bending die was 20 mm, and the tube sizes were as follows: 500 × Φ 8 × t 1, 500 × Φ 12 × t 1, and 500 × Φ 12 × t 2 mm^3. The hollow shapes of the guide and the bending die were determined by the outer contour of the tube, and their gap from the tube was set to be 0.05 mm. According to the principle of flexible-bending, the offset H of the bending die was adjusted as 1, 2, 3, and 4 mm, respectively.

3 Numerical model

In order to study the flexible-bending process of 304 stainless steel tubes, we applied ABAQUS/explicit to numerical simulations (numerical model showed in Fig. 3). The tube was assumed to be isotropic and had an isotropic hardened elastoplastic constitutive behavior. In the material model, it was assumed the material obeyed the von Mises yield criterion. The mechanical properties of 304 stainless steel tube were as follows: density ρ = 7.93 g/cm^3, elastic modulus E = 193 GPa, yield strength σs = 242.31 MPa, Poisson's ratio ν = 0.3, tensile strength σ_b = 694.72 MPa, elongation δ = 40%, and initial size = 500 × Φ 12 × t 2 mm^3. The bending die had thickness of 20 mm and radius of 20 mm. The gap between the guide, the bending die, and the outer contour of the tube was 0.05 mm. The gap between the sleeve and the bending die was

Fig. 2 Jilin University CNC flexible-bending machine

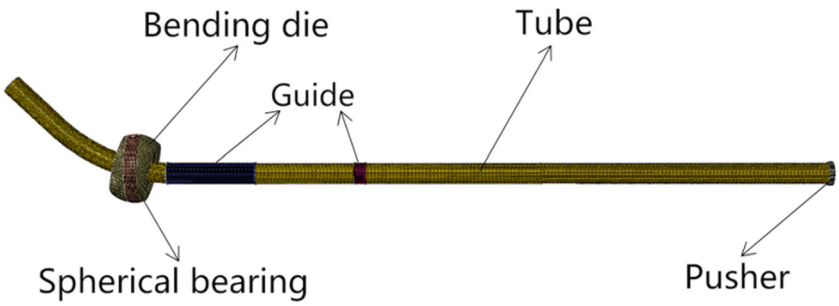

Fig. 3 Finite element model of flexible-bending

0.02 mm. In the forming process, the bending die was modeled with the R3D4 unit, which was the same as the guide devices, ball sets, and pusher that all were discrete rigid bodies. R3D4 is a bilinear quadrilateral 3D rigid element with four nodes. The tubes were modeled with C3D8R units, which are eight-noded hexahedral solid elements with reduced integration. In the finite element model (FEM), the tube was divided by thickness into two layers, and the initial dimension was 1×1 mm^2 in the plate plane and the thickness was 0.5 mm. The friction coefficient was 0.2 for all contact parts. Figure 4 is a graph of the flexible-bending process and shows the relationship among time, tube feed rate, and inclination degree of the bending die.

4 Results and analysis

During the flexible-bending process, the simulations were performed at $H = 3$ mm. Figure 5 shows a schematic view of the half tube. The residual stresses were measured at special positions of the bending tube. The springback was analyzed and optimized using simulation, theory, and experiments.

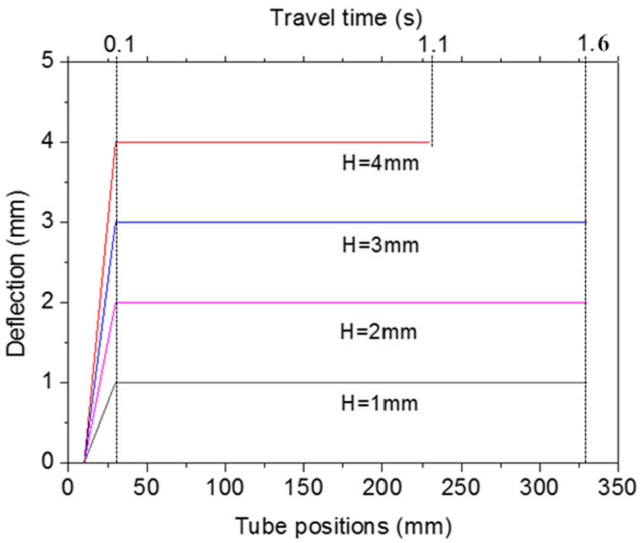

Fig. 4 Process of flexible-bending

4.1 Analysis of residual stresses

During the bending process, the forming quality was represented by some special points. Figure 5 illustrates the relative positions of tube measurement: the residual stresses at axial positions DD1, D′D′1, CC1, C′C′1 and circumferential positions CED, C′E′D′, C1E1D1, C′1E′1D′1 were measured. The wall thickness thinning rate and thickening rate were analyzed. During the bending process, the force of the push block was measured and verified at the stable status.

As shown in Fig. 6, the outer diameter D is 12 mm and wall thickness T is 0.5, 0.6, 0.75, 1, 1.5, and 2 mm, corresponding to the D/T ratio of 24, 20, 16, 12, 8, and 6,

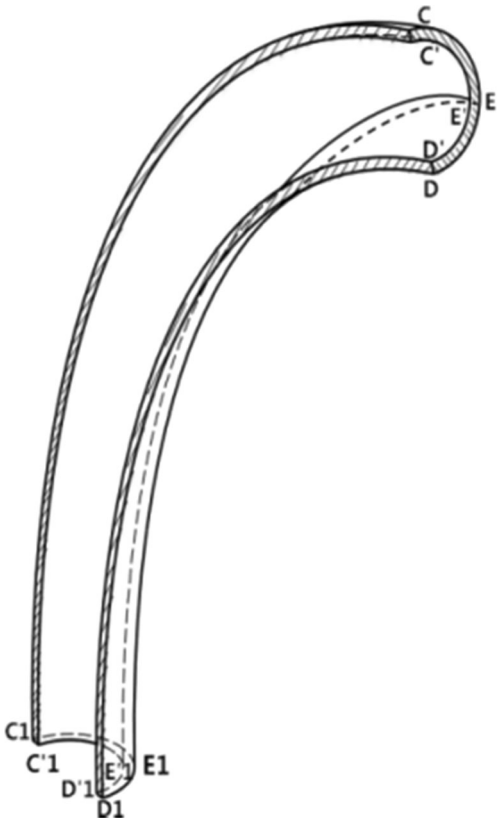

Fig. 5 Measurement position of the tube

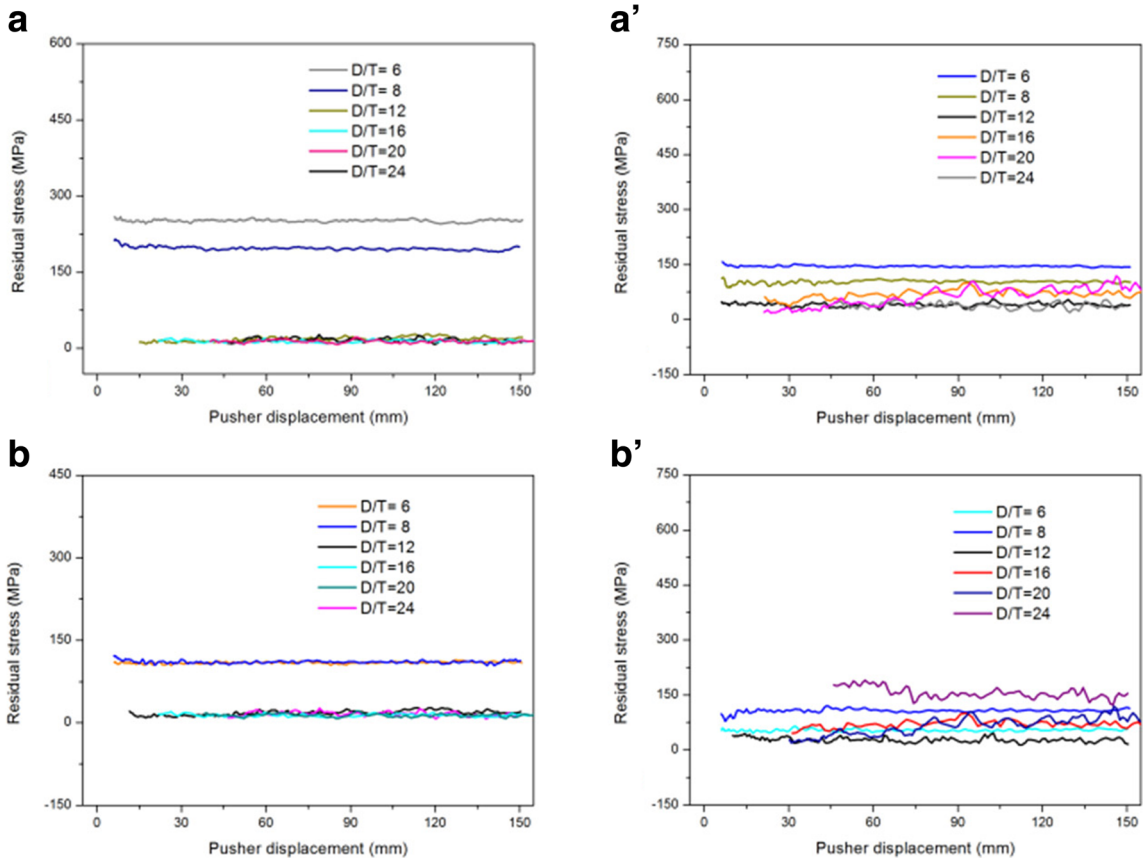

Fig. 6 Effects of wall thickness on residual stress. Residual stress in the special position of the external contour and the hollow inner surface with outer diameter D = 12 mm. Residual stress of paths DD1 (**a**), CC1 (**b**), D′D′1 (**a′**) and C′C′1 (**b′**)

respectively. A variety of tubes were simulated. The special positions of the tubes were measured (Fig. 6). Figure 7 shows a certain wall thickness and varying diameters. Clearly, with the increase of the ratio D/T, the residual stress of the tubes increases first and then decreases (Figs. 6 and 7). In view of the above, regardless of changes in wall thickness or outside diameter, analysis of residual stress indicates the residual stress of tubes first decreases and then increases following the elevation of the ratio D/T. This is very important for the analysis of the forming quality of the tube and contributes to extending its service life.

Figure 8 shows the residual stress map at the circumferential positions. Clearly, when the outer diameter is constant, with the wall thickness decreasing, the residual stresses of the internal and external circumferential directions both decrease, and are evenly distributed.

The target radii of the flexible-bending tubes were consistent, but changed after deformation because of springback. Figure 9 shows the wall thickness changes under constant radius. Data analysis shows the thickening rates of wall thickness T = 0.5, 1, 1.5, and 2 mm are 5.14, 5.1, 3.86, and 4.75, respectively, and the thinning rates are 1.7, 1.83, 1.87, and 1.9%, respectively. Thus, the thickening rates and thinning rates are within the allowable ranges and wall thickness changes remain stable, which modestly guarantee the flexible-bending forming quality.

Figure 10 shows the thrust variation map of push block in the simulation, the outer diameter of the tube is 12 mm, and wall thickness is 1 mm. The thrust of the push block increases with the rise of the offset of the bending die. But from the view that a rising amount of the momentum of the thrust, the thrust wiring increases during the ascending phase of the push block, and finally stabilizes at a certain value. Under the premise of ensuring the geometric accuracy and forming quality, the offset of the bending die is 3 mm and the stability is higher at D/T = 12 (Fig. 11).

4.2 Optimization of the springback

As shown in Fig. 12, H is the Y-direction rise of the bending die when the pusher is fixed; L is the horizontal distance between the right side of the guide device and the gravity center of the bending die; a is the bending angle; and r is the bending radius. At this time, springback did not occur, but would be generated by the profile moving forward in the Z-axis, which was no more obvious after unloading. Thus, in the state of

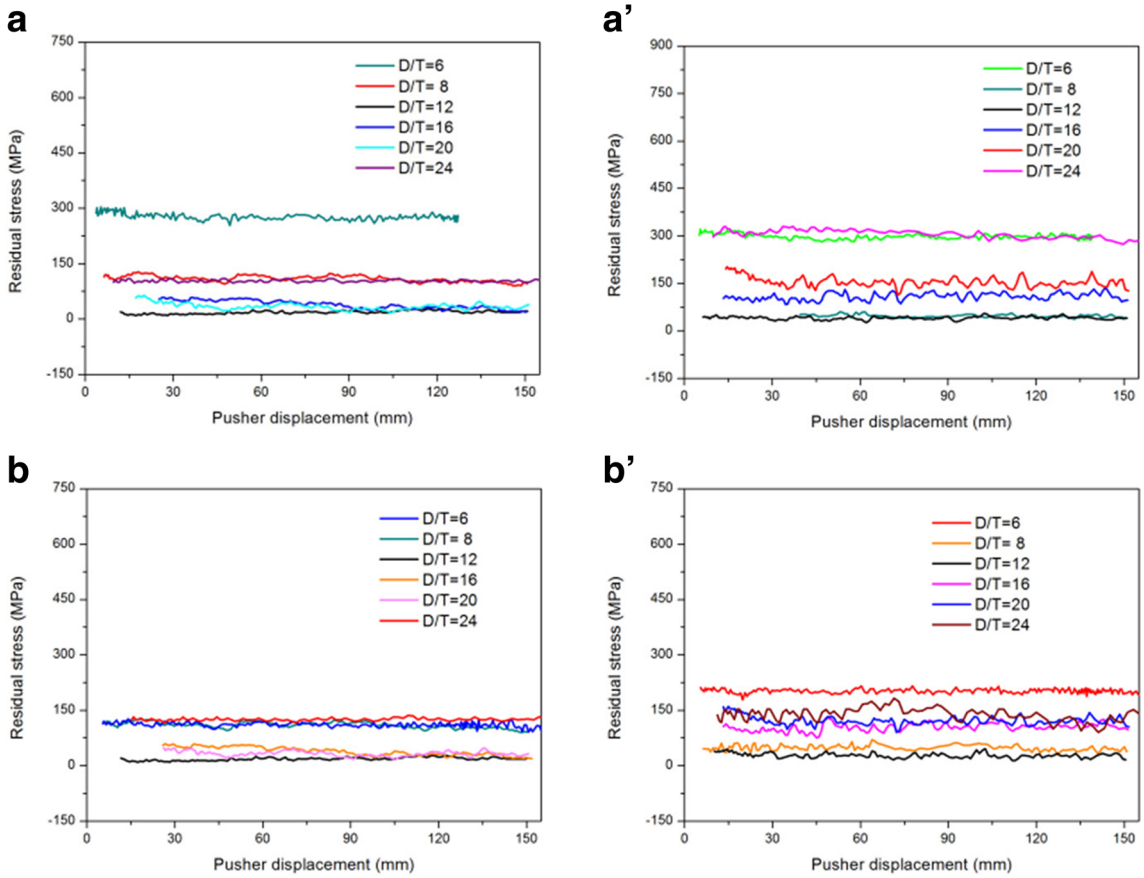

Fig. 7 Effects of outer diameter on residual stress. Residual stress in the special position of the external contour and the hollow inner surface with wall thickness $T = 1$ mm. Residual stress of paths DD1 (**a**), CC1 (**b**), D′D′1 (**a′**), and C′C′1 (**b′**)

Fig. 12, the calculated a and r (the target curvature) are both the theoretical values.

In particular, r and a are computed as follows:

$$\mathrm{r} = \frac{L^2 + H^2}{2H} \tag{1}$$

$$a = \arctan\frac{H}{L} \tag{2}$$

When the tube threaded the bending die at a certain distance, the bending die and the guide device were removed. After unloading, springback occurred. The change of r was

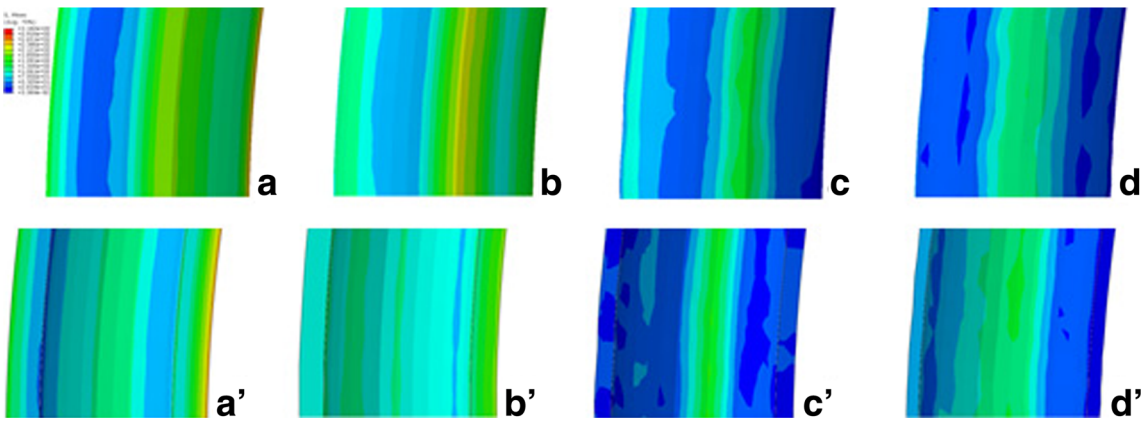

Fig. 8 Circumferential residual stress in $H = 3$ mm. Outer diameter $D = 12$ mm; wall thickness at the external contour and the hollow inner surface $T = 2$ mm (**a**, **a′**), 1.5 mm (**b**, **b′**), 1 mm (**c**, **c′**), and 0.75 mm (**d**, **d′**)

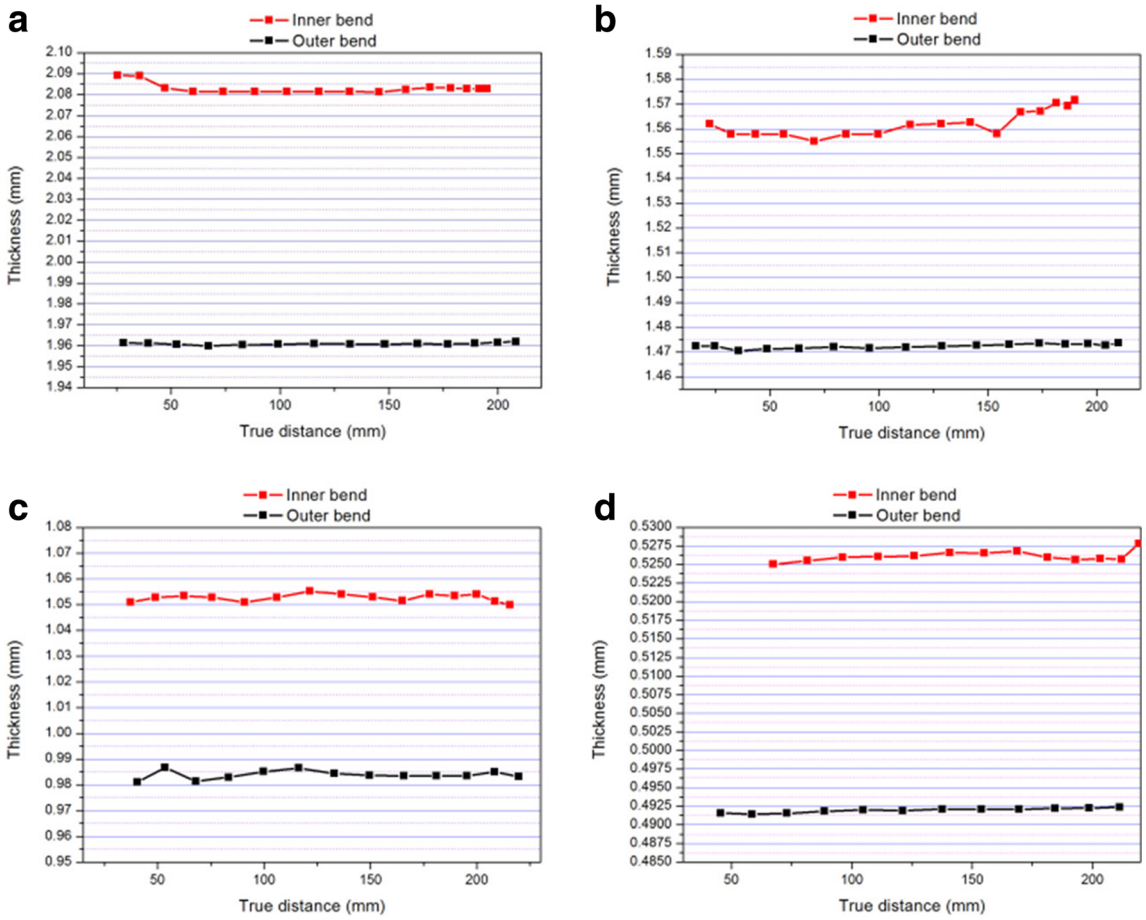

Fig. 9 Comparison of wall thickness. Outer diameter D = 12 mm; original wall thickness T = 2 mm (**a**), 1.5 mm (**b**), 1 mm (**c**), and 0.5 mm (**d**)

estimated by comparing the bending radius at this time (r_0) to the theoretical r.

The bending angle was:

$$a^1 = \arctan\frac{r_0\text{-}\sqrt{r_0{}^2\text{-}L^2}}{L} \tag{3}$$

After unloading, the tube would spring back around the theoretical bending angle, so the springback angle $a_0 = a\text{–}a^1$:

$$a_0 = \arctan\frac{H}{L}\text{-}\arctan\frac{r_0\text{-}\sqrt{r_0{}^2\text{-}L^2}}{L} \tag{4}$$

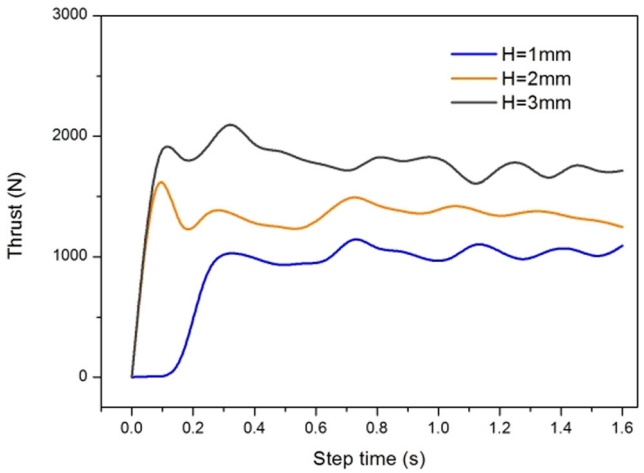

Fig. 10 Thrust of the pusher in H = 1, 2, and 3 mm

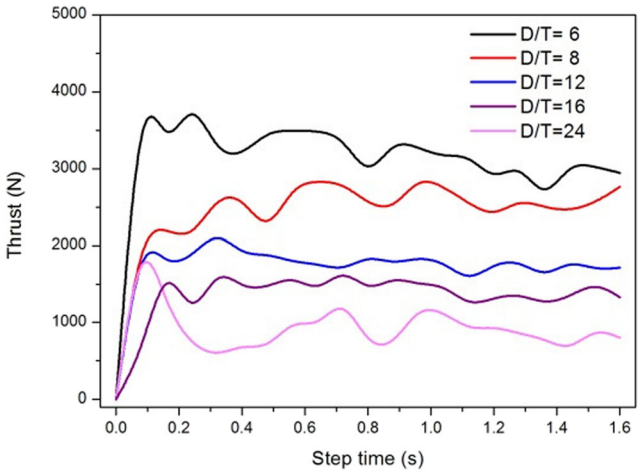

Fig. 11 Thrust of the pusher

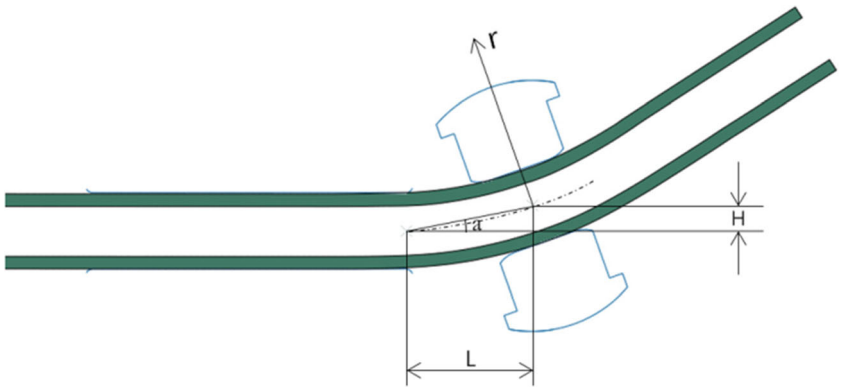

Fig. 12 Size diagram of the flexible-bending model

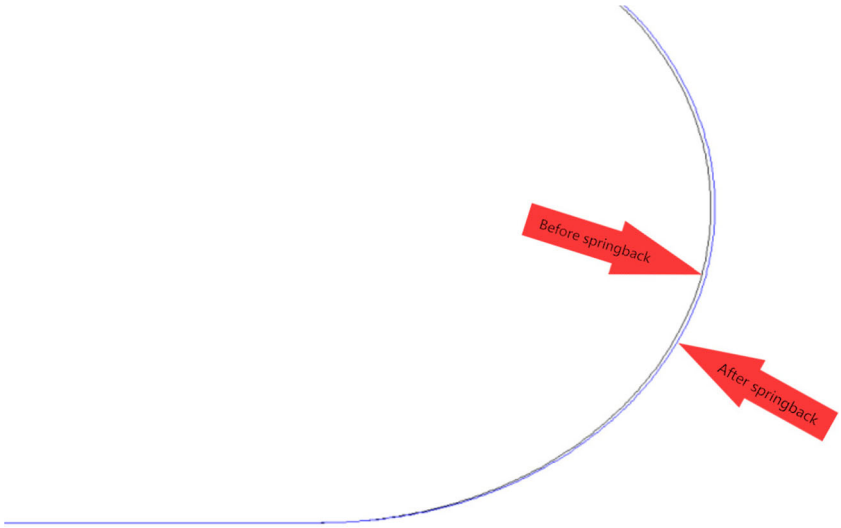

Fig. 13 Springback effect of the neutral layer of the tube

Figure 13 shows the springback effect of the neutral layer of the tube with an outer diameter of 12 mm and a wall thickness of 1 mm. The springback effect can be determined from the relative position of the neutral layer. Figure 14 shows the difference between the theoretical and actual bending angles. Under the conditions of $D = 12$ mm, the curvature increases to a certain value or the curvature of a solid core tube, with the increase of wall thickness. The curvature increases because the tube body volume is enlarged and the plastic behavior surpasses its elastic behavior. As the springback angle

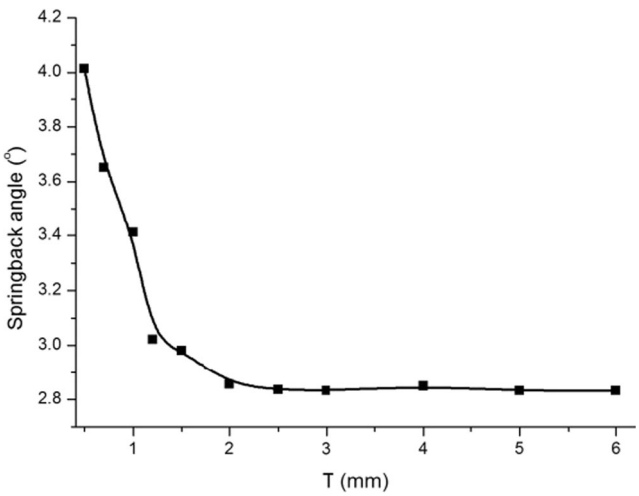

Fig. 14 Effect of the wall thickness on the springback angle

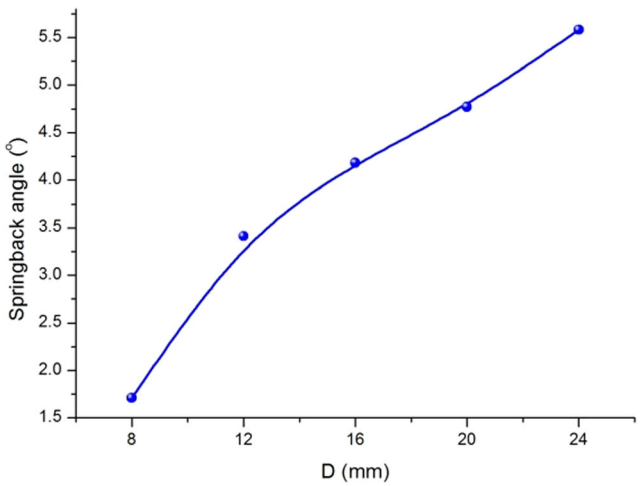

Fig. 15 Effect of the outside diameter on the springback angle

Table 1 Process parameters (L, H). Unit: mm

Target radius R = 68.17 mm	L	20	22	24	25	26	28	30	35	40	45	50
	H	3	3.6477	4.365	4.75	5.153	6.016	6.9564	9.67	12.97	16.964	21.834

decreases, the springback is weakened. Figure 15 shows the relationship between the outer diameter and the difference under the condition of T = 1 mm. With the increase of the outer diameter, the curvature decreases, or namely, the physical material volume of the tube is relatively narrowed down. As the bending radius decreases, the angle and magnitude of springback are enhanced.

The impacts of geometric parameters (outer diameter and wall thickness) on the springback were analyzed. To reduce the impact of springback on the forming part of the target, or the specified radius of curvature, we studied the parameter adjustment in the flexible-bending process, under the premise of certain target radius. The radius of curvature of the target forming part is 68.17 mm. The process parameters are shown in Table 1. From Eq. (1), while L is given, the corresponding H is obtained for the consistency of the target radius.

By adjusting the process parameters L and H, they were matched according to Eq. (1). The experimental and simulation results (Fig. 16): with the increase of L, the actual forming radius gradually approaches the target radius, that is, the springback is successfully weakened. This is because with the increase of L, the theoretical bending angle a increases accordingly. Figure 17 reflects this rule more intuitively, and with the increase of L, the springback angle linearly decreases, which provides a basis for controlling the range of springback.

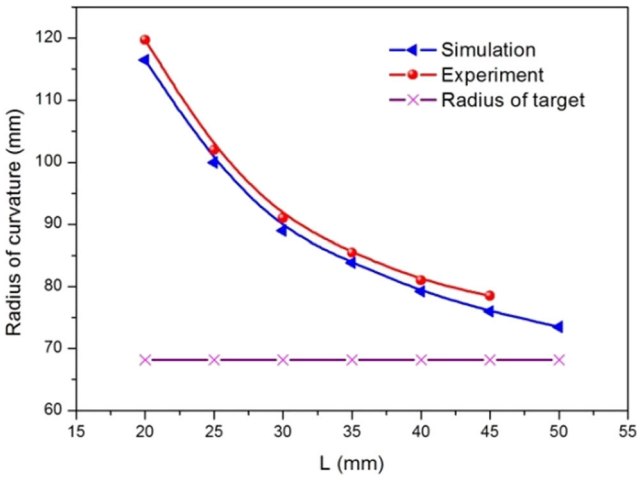

Fig. 16 Comparison of forming radius and target radius

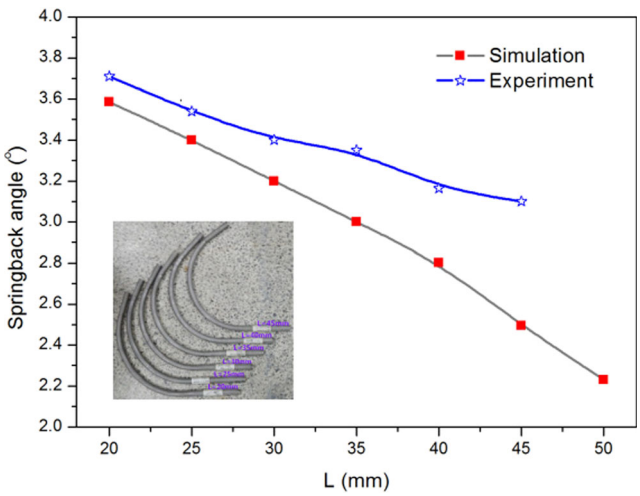

Fig. 17 Springback angle of different L values

5 Conclusions

We investigated the effects of residual stress and springback on the forming quality and geometric accuracy of 304 stainless steel bent tubes. The effects of offsets and wall thickness on residual stress were studied. The wall thickness thickening and thinning rates are also determined. We researched the impacts of outer diameter and wall thickness on springback. The adjustment of process parameters leads to weakened springback according to a certain law, which makes the forming parts closer to the target radius and thus improves the geometric accuracy.

1. A variety of 304 stainless steel tubes are involved in flexible-bending tests. Analysis of residual stress, reduction rate, and stability of the pushing force proves the tubes can be well shaped upon the flexible-bending equipment. Regardless of the change in wall thickness or outer diameter, with the increase of the outer diameter and wall thickness ratio D/T, the axial and circumferential residual stresses of the tubes decrease first and then increase, but neither the thickening rate nor thinning rate is affected by wall thickness changes.
2. During the flexible-bending process, the simulations and experiments were carried out on the basis of theoretical analyses of the springback. Different wall thickness and outer diameters modestly impact the springback. Under the certain law, the L and H are adjusted and both increase, and thereby the springback is optimized. The experiments agree well with the numerical simulations.

Acknowledgements The authors would like to thank professor Mingzhe Li, the founder of China Multi-Point Forming Technology, for his provision of flexible forming equipment and financial support.

References

1. Li H, Yang H, Liu K (2013) Towards an integrated robust and loop tooling design for tube bending. Int J Adv Manuf Technol 65:1303–1318. https://doi.org/10.1007/s00170-012-4258-1
2. Liang JC, Song G, Fei T, Yu PZ, Song XJ (2014) Flexible 3D stretch-bending technology for aluminum profile. Int J Adv Manuf Technol 71:1939–1947. https://doi.org/10.1007/s00170-013-5590-9
3. Corona E (2004) Simple analysis for bend-stretch forming of aluminum extrusions. Int J Mech Sci 46:433–448. https://doi.org/10.1063/1.1766680
4. Murata M, Kuboki T (2015) CNC tube forming method for manufacturing flexibly and 3-dimensionally bent tubes. Springer, Berlin, pp 363–368. https://doi.org/10.1007/978-3-662-46312-3_56
5. Hermes M, Chatti S, Weinrich A et al (2008) Three-dimensional bending of profiles with stress superposition. Int J Mater Form 1(1):133–136. https://doi.org/10.1007/s12289-008-0 -0
6. Strano M, Colosimo BM, Castillo ED (2011) Improved design of a three roll tube bending process under geometrical uncertainties. AIP Conf Proc 1353(1):35–40. https://doi.org/10.1063/1.3589488
7. Gemignani R, Strano M. US patent US 8141403 B2
8. Vatter PH, Plettke R (2013) Process model for the design of bent 3-dimensional free-form geometries for the three-roll-push-bending process. Procedia Cirp 7(5):240–245. https://doi.org/10.1016/j.procir.2013.05.041
9. Gantner P, Bauer H, Harrison DK et al (2005) Free-bending—a new bending technique in the hydroforming process chain. J Mater Process Technol 167(2–3):302–308. https://doi.org/10.1016/j.jmatprotec.2005.05.052
10. Li P, Wang L, Li M (2016) Flexible-bending of profiles and tubes of continuous varying radii. Int J Adv Manuf Technol. https://doi.org/10.1007/s00170-016-8885-9
11. Murata M, Ohashi N, Suzuki H (1989) New flexible penetration bending of a tube: 1st report, a study of MOS bending method. Trans Jpn Soc Mech Eng C 55:2488–2492. https://doi.org/10.1299/kikaic.55.2488
12. Murata M (1996) Effects of inclination of die and material of circular tube in MOS bending method. Trans Jpn So Mech Eng C 62:3669–3675. https://doi.org/10.1299/kikaic.62.3669
13. Murata M (1996) Effect of die profile and aluminum circular tube thickness with MOS bending. J Jpn Inst Light Met 46:626–631. https://doi.org/10.2464/jilm.46.626
14. Li P, Wang L, Li M (2016) Flexible-bending of profiles with asymmetric cross-section and elimination of side bending defect. Int J Adv Manuf Technol 87:2853–2859. https://doi.org/10.1007/s00170-016-8673-6
15. Strano M (2005) Automatic tooling design for rotary draw bending of tubes. Int J Adv Manuf Technol 26:733–740. https://doi.org/10.1007/s00170-003-2055-6
16. Zhao GY, Liu YL, Yang H (2010) Effect of clearance on wrinkling of thin-walled rectangular tube in rotary draw bending process. Int J Adv Manuf Technol 50:85–92. https://doi.org/10.1007/s00170-009-2508-7
17. Gantner P, Harrison DK, Silva AKMD, Bauer H (2004) New bending technologies for the automobile manufacturing industry. Proc Int Matador Conf 211-216. https://doi.org/10.1007/978-1-4471-0647-0_32
18. Gantner P, Harrison DK, De Silva AK, Bauer H (2007) The development of a simulation model and the determination of the die control data for the free-bending technique. Proc Inst Mech Eng B J Eng Manuf 221:163–171. https://doi.org/10.1243/09544054JEM642